The Astrophysical Journal, 615:526–530, 2004 November 1

RADIO OBSERVATION OF ELECTRON ACCELERATION AT SOLAR FLARE RECONNECTION OUTFLOW TERMINATION SHOCKS

Henry Aurass and Gottfried Mann
Astrophysikalisches Institut Potsdam, An der Sternwarte 16, D-14482 Potsdam, Germany; haurass@aip.de
Received 2004 February 15; accepted 2004 July 11

ABSTRACT

Using meter-wave solar radio spectral observations of the 2001 September 28 flare, we discuss simultaneously appearing type II–like bursts observed at 40–80 MHz and ≈300 MHz as radio signatures of the upper and lower reconnection outflow termination shock (TS). The features are identified during the impulsive phase but well after the regular traveling-shock type II burst and during the rise of a coronal mass ejection. The upper and lower TS features reveal a tendency for flux anticorrelation over time. We use radio imaging data (Nançay Radio Heliograph) and *Yohkoh* soft X-ray images to support the TS hypothesis. Assuming shock drift acceleration, we compute the flux of accelerated electrons for lower TS conditions that lead to an electron population with energies of ≈15 keV.

Subject headings: acceleration of particles — MHD — shock waves — Sun: flares — Sun: radio radiation

1. INTRODUCTION

Meter-wave radio burst observations reflect the dynamics of nonthermal energy release (electron acceleration) during solar flares. The reconnection model of flare energy release (e.g., Priest & Forbes 2000; Kosugi & Somov 1998) predicts hot reconnection outflow jets surrounded by a system of standing slow-mode shocks in the corona. In the jets, standing fast-mode shocks (called termination shocks [TSs]) are expected somewhere between the diffusion region (DR) and the erupting prominence (upper TS), and between the DR and the top of the postflare loops (lower TS; see Fig. 1).

Fast-mode shocks are usually able to generate energetic electrons and thus possibly also radio emission. Aurass et al. (2002) identified a TS radio signature about 30 minutes after the impulsive flare phase. Several authors (e.g., Shibata et al. 1995; Tsuneta & Naito 1998) invoked the lower TS to explain the hard X-ray loop-top source of flares. Electron acceleration at the TS in the reconnection geometry is of general astrophysical interest. Therefore, in the present paper we consider two questions:

1. Can TS signatures be observed in dynamic radio spectra as early as the impulsive phase of solar flares?
2. How much energy can electrons gain in such a configuration?

2. OBSERVATION OF UPPER AND LOWER TS RADIO SIGNATURE

Figure 2 shows the radio spectrum of the 2001 September 28 flare[1] recorded at the Astrophysical Institute of Potsdam (AIP), Tremsdorf Observatory. This event is associated with a coronal mass ejection (CME) seemingly starting near the active region and during the impulsive flare phase (2001 *SOHO* LASCO CME archive).

Among other signatures the spectrum contains (at about 8:20 UT) a "regular" type II burst with the characteristic fundamental-harmonic (FH) and split-band pattern. In dynamic radio spectra, a type II burst is a narrowband signature drifting slowly from high to low frequencies. Most coronal type II bursts are excited by traveling coronal shocks (e.g., Nelson & Melrose 1985). Sometimes "herringbone" spectral fine structures appear as rapidly drifting emission stripes leaving type II lanes toward high and low frequencies. They provide evidence of electron acceleration at the traveling disturbance (Cairns & Robinson 1987). For the regular type II burst in Figure 2 we derive a shock exciter speed of about 810 km s^{-1} from its frequency drift rate using a fourfold Newkirk (1961) coronal density model.[2] The accompanying CME reveals a similar propagation speed of 846 km s^{-1} (2001 *SOHO* LASCO CME archive).

Roughly 4 minutes after the regular type II burst the whole 40–800 MHz range shows continuum emission superposed with even slower drifting narrowband features between 40 and 80, as well as 280–380 MHz. This means we observe a sequence of two distinct nonthermal energy release signatures in radio emission. The *GOES* 0.5–4 Å soft X-ray flux and its time derivative[3] (positive values are overplotted in Fig. 2; negative values are omitted) confirm a corresponding sequence of two energy release stages.

After 8:30 UT, the FH–related features between 40 and 80 MHz strongly suggest a further regular type II burst. The drift rate corresponds to speeds of 0–100 km s^{-1}. We call it an "upper TS" feature. Simultaneously, a narrowband nondrifting lane occurs near 300 MHz. Sometimes it shows the usual type II burst features such as band split and herringbones. Between 08:40 and 08:50 UT this lane drifts toward lower frequencies pointing to a speed between 35 and 60 km s^{-1}. After 08:50 UT the event decays. We call this feature "lower TS."

Note that the upper and lower TS radio emissions are in no way harmonically related. However, if we plot the flux-time dependence, (in Fig. 2, along the dotted lines) we find some similarity between the two patterns (Fig. 3) starting at least after 08:35 UT. Considering both flux records as a sequence of pairwise associated measurements, we obtain a significantly nonzero

[1] Onset at N10, E18 at 08:10 UT, Hα/X-ray importance ratings 2N/M3.3, according to NOAA Solar Geophysical Data 2001.

[2] The same model is generally applied here below.

[3] Used as a proxy of the hard X-ray flux—the Neupert effect, e.g., Veronig et al. (2002).

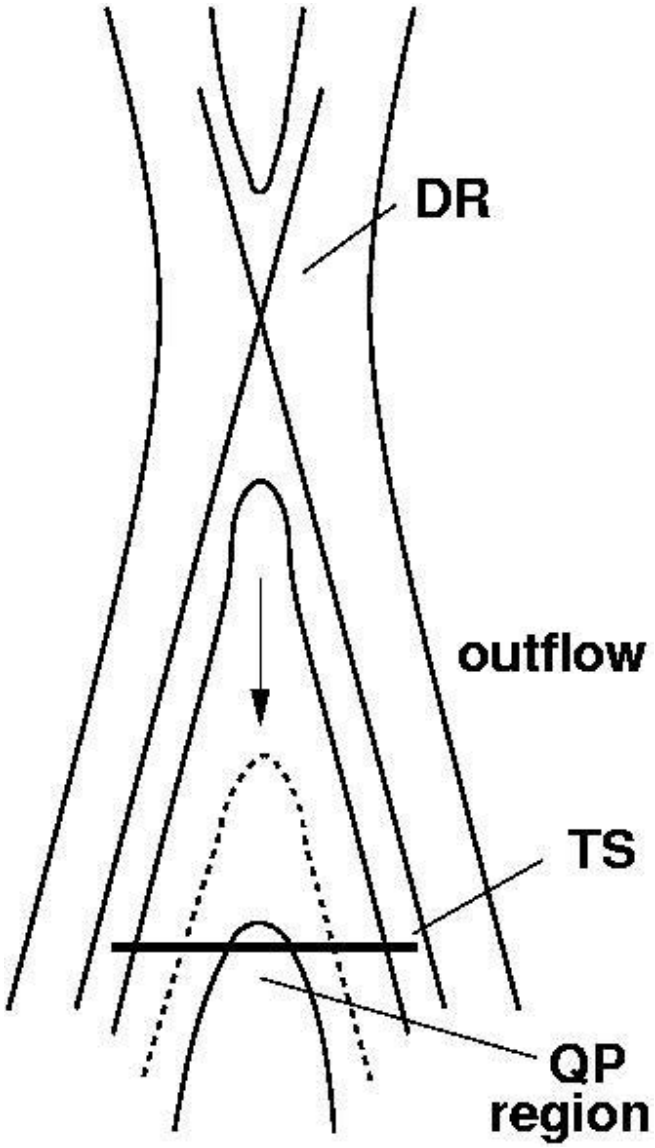

FIG. 1.—Position of the lower TS in the outflow region. The diffusion region is labeled "DR," and the quasi-perpendicular shock region is labeled "QP."

rank correlation coefficient[4] of −0.26, revealing that to a certain extent rising 58 MHz flux values are associated with falling 327 MHz flux values and vice versa. We interpret this as both records having a tendency toward anticorrelation.

In Figure 4 we used Nançay Radio Heliograph (NRH) data to compare the radio source centroids of the lower TS feature with simultaneously observed *Yohkoh* soft X-ray telescope images. The SXT Be119 filter is sensitive to the upper temperature range in the flare plasma (>10^7 K). Only because of the identification of the TS features in the radio spectrum (Fig. 2) do we know that the NRH 327 MHz record represents the lower TS source well. Figure 4 reveals that the lower TS source is really situated above the flaring active region near a cusplike structure on top of hot and dense (X-ray visible) loops. The upper TS source site cannot be similarly shown.[5]

In addition to the radio spectrum, the soft X-ray flux in Figure 2 suggests an association of both TS features with a reactivation of flare energy release. From inspection of *Yohkoh* soft X-ray and NRH radio images, we obtained for the lower TS feature a position of the radio source over the bright X-ray arcade, quite in accord with magnetic reconnection as an energy-release process. The anticorrelation tendency between the (representatively selected) radio flux levels at 58 and 327 MHz (Fig. 3) points to a causal connection between widely separated height (density) levels in the corona.

In principle, at least the upper TS feature might be caused by the propagating CME. It is widely accepted that both CME leading edge–driven bow shocks and CME flank–driven bow shocks are possible. Note that the flare-associated CME is observed with its fastest leading edge at 3 $R_\odot$ at 08:54 UT. Therefore, in the given case we believe that the CME significance for radio spectrum interpretation is improbable but cannot be ruled out with certainty.

We note that the fast-mode termination shock simulations of Forbes (1986; see his Fig. 2) yield a fluctuating but related behavior of the strength of the upper and lower TS. With due caution it seems that these model calculations predict the observed behavior if we associate the shock strength with the escaping radio flux.

3. ELECTRON ACCELERATION BY FLARE TS

In such configurations the observed radio signatures of TS require electron acceleration. Now we discuss a plausible mechanism. As sketched in Figure 1, the reconnected magnetic field is convected away from the DR in the outflow region.

Therefore, the TS becomes quasi-perpendicular (QP) in a certain range (QP region in Fig. 1). In this region the angle $\theta_{B,n}$ between the normal to the shock and the upstream magnetic field is greater than 45°, and electrons can be efficiently accelerated by shock drift acceleration (Holman & Pesses 1983; Ball & Melrose 2001). Their velocity gain parallel to the upstream magnetic field is $V_{r,\parallel} = 2v_s \sec\theta_{B,n} - V_{i,\parallel}$ because of the reflection at the shock, whereas the velocity component perpendicular to the upstream magnetic field remains unchanged, i.e., $V_{r,\perp} = V_{i,\perp}$. Here i and r denote the velocity component before and after the reflection at the shock and v_s is the shock speed. Then, according to Leroy & Mangeney (1984) and Wu (1984), the accelerated electrons establish a so-called shifted loss-cone velocity distribution function in the upstream region:

$$f_{\rm acc} = \Theta\left(V_\parallel - v_s \sec\theta_{B,n}\right) \times \Theta\left(V_\perp - \left[\tan\alpha_{\rm lc}\sqrt{\left(V_\parallel - v_s\sec\theta_{B,n}\right)^2 + \frac{2e\phi}{m_e}}\right]\right) \times f_0\left(2v_s\sec\theta_{B,n} - V_\parallel,\ V_\perp\right). \quad (1)$$

Here m_e is the electron mass, f_0 is the initial velocity distribution function, and $\Theta(x)$ is the step function. The term $e\phi = [\gamma/(\gamma-1)]k_{\rm B}T[(N_{\rm down}/N_{\rm up})^{\gamma-1} - 1]$ denotes the cross-shock potential (Goodrich & Scudder 1984). The loss-cone angle $\alpha_{\rm lc}$ is defined by $\alpha_{\rm lc} = \arcsin[(B_{\rm up}/B_{\rm down})^{1/2}]$. $N_{\rm down}/N_{\rm up}$ and $B_{\rm down}/B_{\rm up}$ are the ratios of density and magnetic field compression at the shock. If we assume a Maxwellian distribution,

$$f_0\left(V_\parallel,\ V_\perp\right) = \left(2\pi v_{\rm th}^2\right)^{-3/2}\exp\left[-\left(V_\parallel^2 + V_\perp^2\right)/2v_{\rm th}^2\right],$$

with the thermal speed $v_{\rm th} = (k_{\rm B}T/m_e)^{1/2}$ (where $k_{\rm B}$ is Boltzmann's constant, T is the temperature, and m_e is the electron

[4] Significance of 6.2×10^{-9} on a scale of 0–1, where zero means significant; see IDL routine *r_correlate*.

[5] No radio imaging is available below 160 MHz.

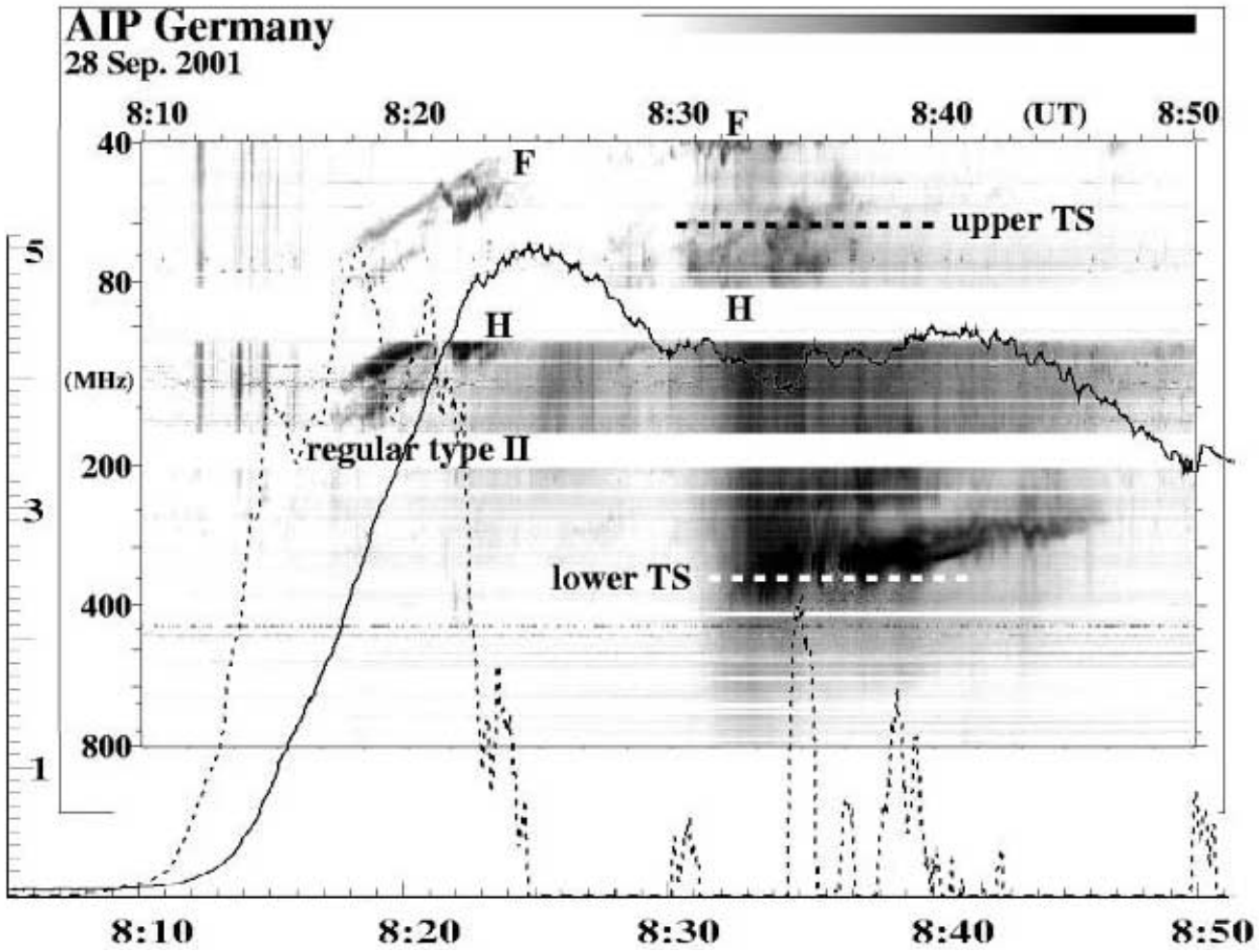

FIG. 2.—The 40–800 MHz radio spectrum of the 2001 September 28 event observed at AIP. White gaps in the frequency range are due to terrestrial transmitters. *GOES* 0.5–4 Å flux (*solid line*) and, where positive, its time derivative (*dotted line*) are overplotted. Flux ordinate units are 10^{-6} W m^{-2}. The derivative is on an arbitrary scale.

mass), as the initial state in the upstream region, the fluxes of accelerated electrons can conventionally be determined by

$$d\Phi = 2\pi f_{\rm acc} V^3 \sin\theta \, d\theta \, dV, \qquad (2)$$

with $V = (V_\perp^2 + V_\parallel^2)^{1/2}$. Here θ denotes the electron pitch angle $\theta = \arctan(V_\perp / V_\parallel)$. In the nonrelativistic case, i.e., for electrons with energies less than 60 keV, V is usually related to the energy by $V = (2E/m_e)^{1/2}$.

To relate these results to our observations, an electron number density $N_e = 10^9$ cm^{-3} and a magnetic field of $B = 10$ G are adopted as plasma parameters at the 300 MHz level in the corona near the lower TS. A temperature of 10^7 K is used for the flare plasma. We obtain a thermal electron speed of 12,300 km s^{-1} and an Alfvén speed of 670 km s^{-1}. In addition, we assume $N_{\rm down}/N_{\rm up} = B_{\rm down}/B_{\rm up} = 2$ for the jump of the density and magnetic field across the TS. This leads to an Alfvén Mach number of 2.32 (i.e., a shock speed $v_s = 1600$ km s^{-1}) according to the Rankine-Hugoniot relations. The differential fluxes defined by the ratio $j = d\Phi/dE$ of energetic electrons calculated by equation (2) after integrating over the pitch angles θ are plotted for two angles $\theta_{B,n}$ in Figure 5. Evidently, for $\theta_{B,n} = 88^\circ$, the TS produces an electron population with an energy of about 15 keV by shock drift acceleration. In this case, 4% of all electrons in the upstream region are accelerated, but they carry 64% of the energy of all electrons there. If the angle $\theta_{B,n}$ approaches 90°, the shock speed $v_s \sec\theta_{B,n}$ exceeds the velocity of light in the de Hoffmann–Teller frame. In our case that happens at 89°.7 for $v_s = 1600$ km s^{-1}. For angles larger than 89°.7, no de Hoffmann–Teller frame exists. In the case of $\theta_{B,n} = 90^\circ$ no magnetic field line connects the upstream with the downstream region; i.e., the shock can never reflect a charged particle back to the upstream region.[6]

Since this occurs at the QP region of the TS (see Fig. 1) the reflected electrons again reach the TS after traveling a short distance because of the strong magnetic field line curvature there. However, now most of them pass through the TS into the downstream region since they have experienced a strong decrease of pitch angle caused by the initial reflection at the shock. Because of their further movement along the (downstream) magnetic field, the energetic electrons finally reach denser regions in the low corona, where they generate X-rays via bremsstrahlung emission.

Thus, depending on the local magnetic field topology, TS-accelerated electrons can be responsible for *both* the hard X-ray loop-top *and* loop-footpoint sources. Further, it should also be emphasized that the upper TS is able to accelerate

[6] A detailed discussion of shock drift acceleration for superluminal shocks is given by Begelmann & Kirk (1990).

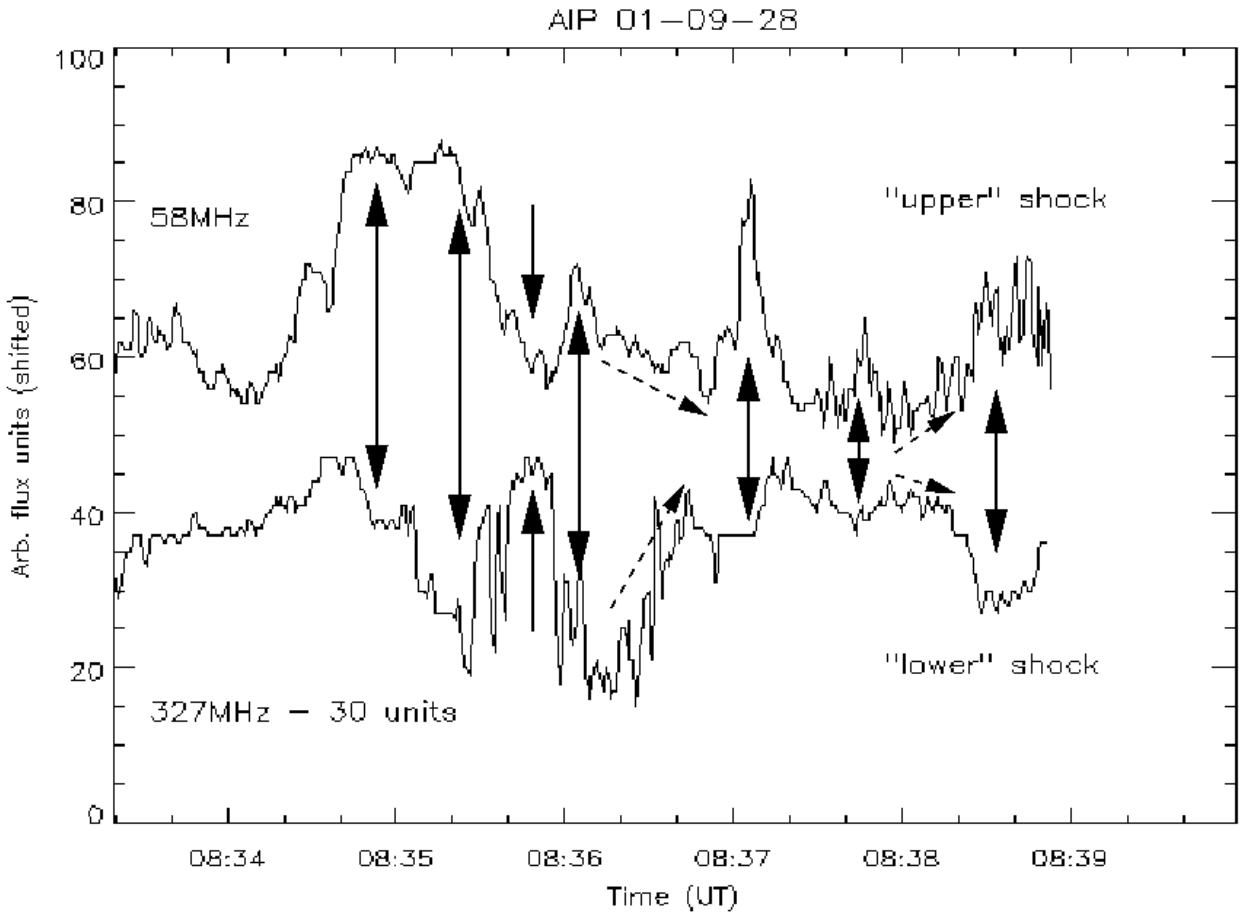

FIG. 3.—The 327 and 58 MHz flux records derived from the spectrum in Fig. 2. As a formal measure of similarity, we determined a highly significant rank corrrelation coefficient of −26%. The arrows indicate the tendency of anticorrelation between the two records.

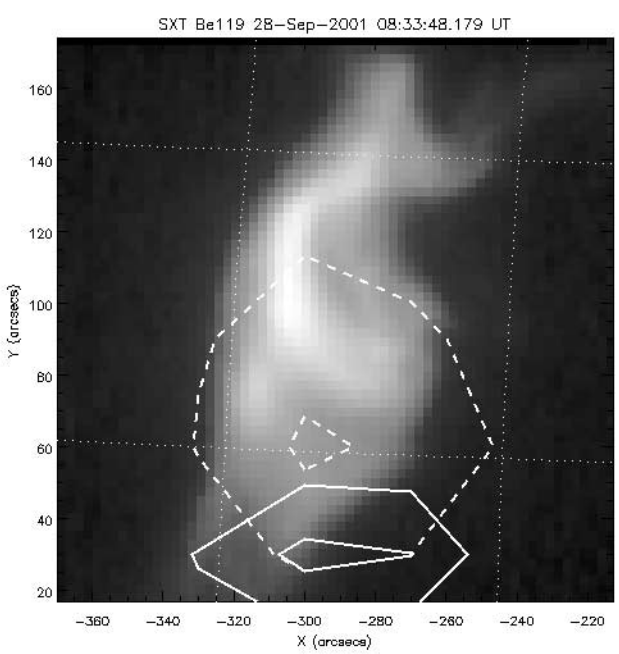

FIG. 4.—*Yohkoh* SXT image (Be119; mean of 08:33:48–08:37:44 UT; hot and dense features appear white) with superposed radio emission isolines (NRH data, courtesy of the NRH Group). We show 327 MHz (98% and 93% of maximum) data for 08:39:50 (*solid contours*) and 08:42 UT (*dotted contours*).

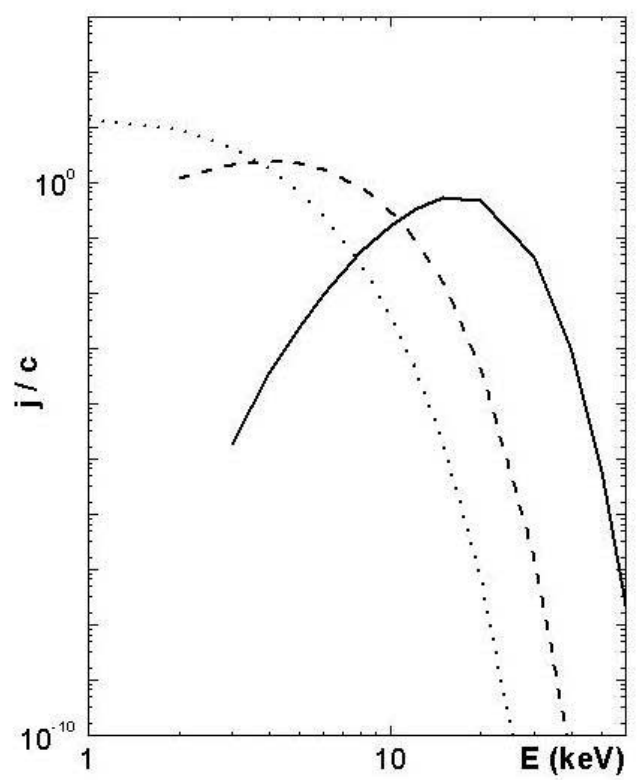

FIG. 5.—Differential electron flux as a function of energy in keV according to eq. (1), for $\theta_{B,n} = 85°$ (*dashed line*) and 88° (*solid line*). The dotted line represents the Maxwellian with 10^7 K. True fluxes are obtained by $(j/c)5.86 \times 10^{16}$ (keV cm^2 s)$^{-1}$.

electrons via the same mechanism. It is a candidate for the region that excites low-frequency fast drift (type III) bursts. Finally, we note that the invoked mechanism (shock drift acceleration) would also be able to accelerate protons, thus leading to an enhanced proton flux at ≈30 MeV.

We acknowledge the use of the publicly available data of the Nançay Radio Heliograph and the *Yohkoh* and *GOES* space observatories, as well as the *SOHO* LASCO CME listings. We are grateful to B. Vršnak and A. Warmuth for discussions about magnetic reconnection and solar flares.

REFERENCES

Aurass, H., Vršnak, B., & Mann, G. 2002, A&A, 384, 273
Ball, L., & Melrose, D. B. 2001, Publ. Astron. Soc. Australia, 18, 361
Begelmann, M. C., & Kirk, J. G. 1990, ApJ, 353, 66
Cairns, I. H., & Robinson, R. D. 1987, Sol. Phys., 111, 365
Forbes, T. 1986, ApJ, 305, 553
Goodrich, C. C., & Scudder, J. 1984, J. Geophys. Res., 89, 6654
Holman, G. D., & Pesses, M. E. 1983, ApJ, 267, 837
Kosugi, T., & Somov, B. V. 1998, in Observational Plasma Astrophysics: Five Years of *Yohkoh* and Beyond, ed. T. Watanabe, T. Kosugi, & A. Sterling (Boston: Kluwer), 297
Leroy, M. M., & Mangeney, A. 1984, Ann. Geophys., 2, 449
Nelson G. S., & Melrose, R. D. 1985, in Solar Radiophysics: Studies of Emission from the Sun at Metre Wavelengths, ed. D. J. Mclean & N. R. Labrum (Cambridge: Cambridge Univ. Press), 333
Newkirk, G. A. 1961, ApJ, 133, 983
Priest, E., & Forbes, T. 2000, Magnetic Reconnection: MHD Theory and Applications (New York: Cambridge Univ. Press)
Shibata, K., Masuda, S., Shimojo, M., Hara, H., Yokoyama, T., Tsuneta, S., Kosugi, T. & Ogawara, Y. 1995, ApJ, 451, L83
Tsuneta, S., & Naito, T. 1998, ApJ, 495, L67
Veronig, A., Vršnak, B., Dennis, B. R., Temmer, M., Hanslmeier, A., & Magdalenic, A. 2002, A&A, 392, 699
Wu, C. S. 1984, J. Geophys. Res., 89, 8857